Supplementary Materials

Enhancing atomic ordering, magnetic and transport properties of Mn_2VGa Heusler alloy thin films toward negatively spin-polarized charge injection

Z.H. Li[a], H. Suto[a*], V. Barwal[a], K. Masuda[a], T.T. Sasaki[a], Z.X. Chen[a], H. Tajiri[b], L.S.R. Kumara[b], T. Koganezawa[b], K. Amemiya[c], S. Kokado[d], K. Hono[a], Y. Sakuraba[a]

[a] National Institute for Materials Science, 1-2-1 Sengen, Tsukuba, 305-0047, Japan

[b] Japan Synchrotron Radiation Research Institute, 1-1-1 Kouto, Hyogo, 679-5198, Japan

[c] Institute of Materials Structure Science, High Energy Accelerator Research Organization, 1-1 Oho, Tsukuba, 305-0801, Japan

[d]Graduate School of Integrated Science and Technology, Shizuoka University, 3-5-1 Johoku, Shizuoka, 432-8561, Japan

*Corresponding author: suto.hirofumi@nims.go.jp

S.1: Interfacial structure of post-annealed MVG films

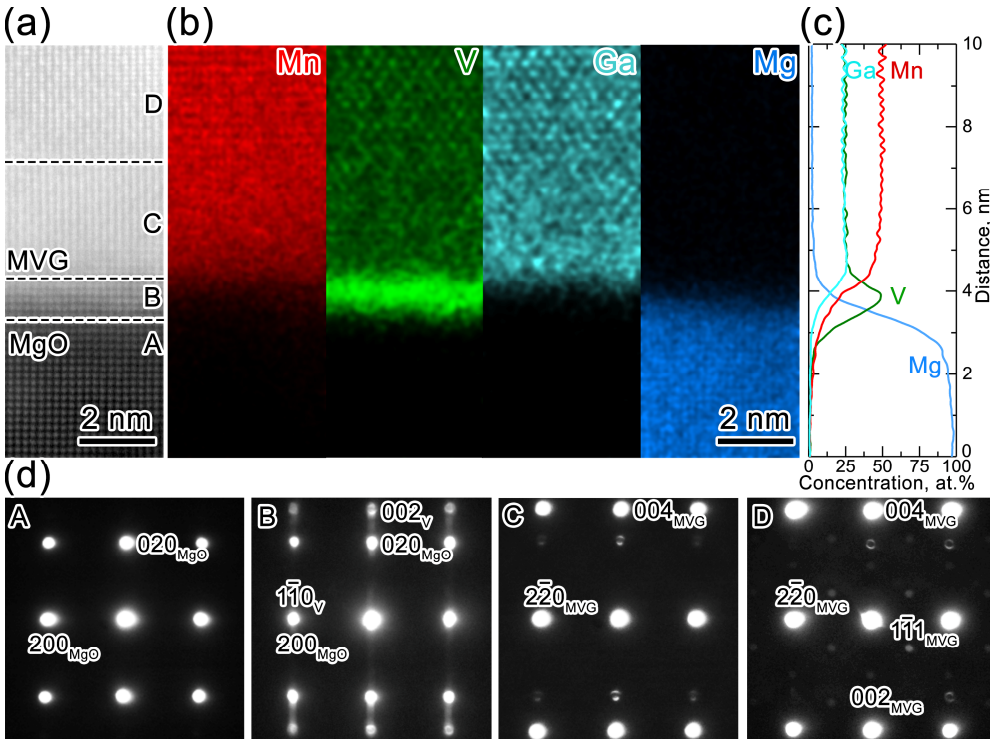

Fig. S.1. (a) Atomic-resolution HAADF-STEM image, and corresponding (b) EDS elemental maps, and (c) compositional line profiles across the post-annealed MgO/Mn_2VGa interface. (d) NBED pattens taken from the Regions A, B, C, and D in (a), respectively.

Figure S.1 shows the post-annealed MgO/Mn_2VGa interface at 600 °C. The atomic-resolution HAADF-STEM image clearly shows a ~ 1 nm-thick interface (Region B) between the MgO and the Mn_2VGa film, **Fig. S.1a**. The EDS elemental maps and corresponding composition line profiles (**Fig. S.1b and 1c**) show that the MgO/Mn_2VGa interface is enriched in V atoms. Combined with a series of NBED patterns taken from MgO (Region A) to Mn_2VGa (Region D), **Fig. S.1d**, a BCC-structured V phase may be formed at the MgO/Mn_2VGa interface with an epitaxial relationship of (001)[110]V // (010)[001]MgO, as previously reported [1,2]. Because pure V is paramagnetic, it has little influence on the magnetic properties of the prepared MVG films.

S.2: Composition dependence of anisotropic magnetoresistance measurements

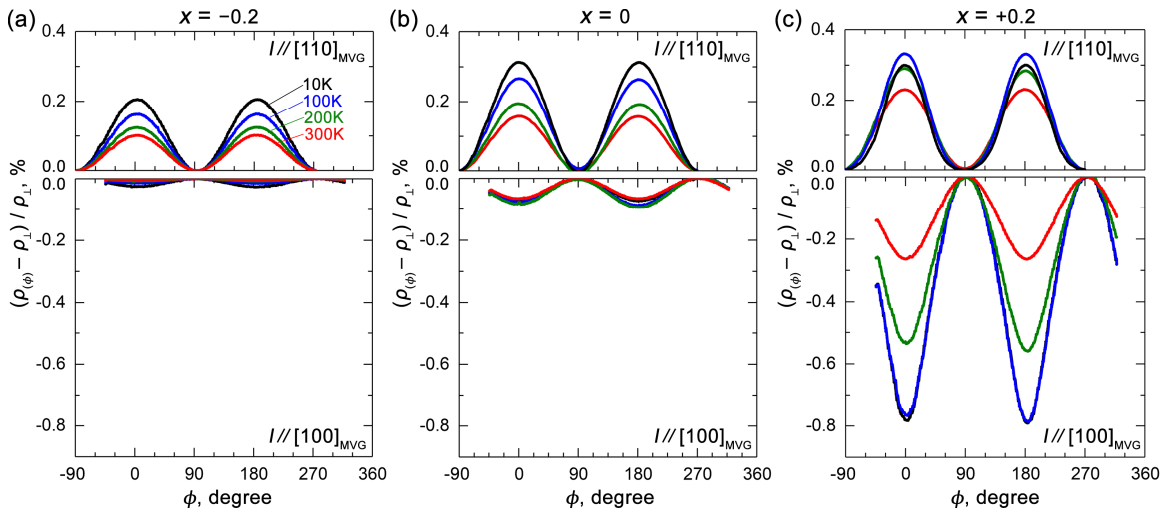

Fig. S.1. The ϕ dependence of the AMR ratio for $Mn_{2+x}V_{1-x}Ga$ films with x = (a) −0.2, (b) 0, and (c) +0.2, respectively. Note that the current directions were aligned along $[110]_{MVG}$

Figures S.2a-c shows the AMR ratio as a function of ϕ for $Mn_{2+x}V_{1-x}Ga$ (x = −0.2, 0, +0.2) films measured from 10 to 300 K. All MVG films exhibit positive AMR ratios for the current along the $[110]_{MVG}$, and negative ratios as the current direction aligned with the $[100]_{MVG}$. The magnitude of negative AMR ratios along the $[100]_{MVG}$ shows a strong composition dependence. The AMR ratio increases with increasing the x and is dramatically enhanced at x = +0.2, which

implies the changes in the electronic band structure with the composition. However, a detailed analysis on the composition dependence of AMR is beyond the scope of this study, and we primarily focus on the stoichiometric sample as discussed in the main text.

S.3: Theoretical analysis of anisotropic magnetoresistance results

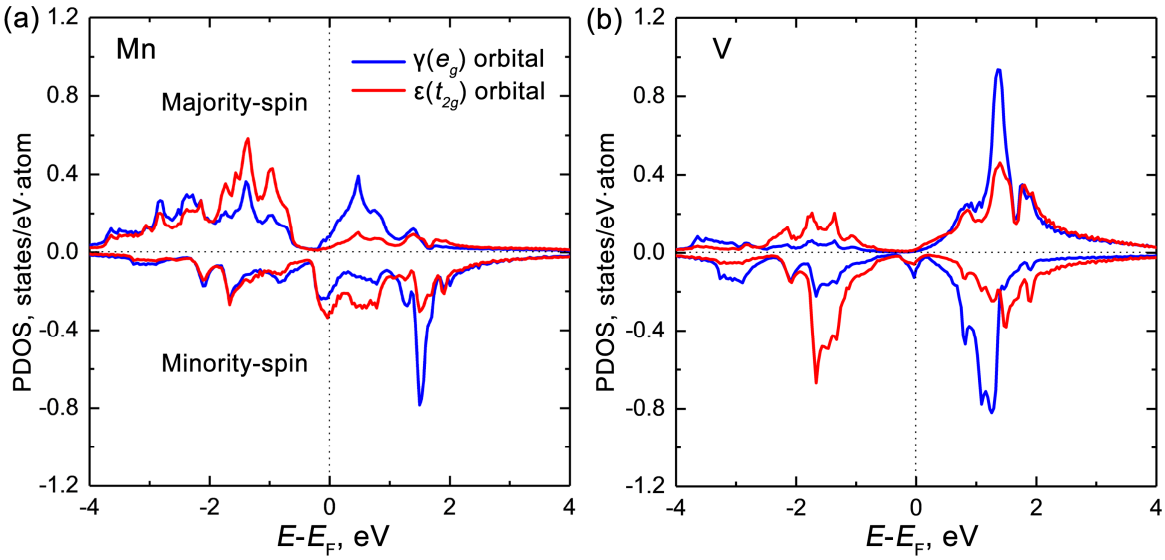

In theoretical calculations of AMR in Mn_2VGa (x = 0), we consider that Mn atoms dominate the *s*–*d* scattering process because the *d*-orbital density of states (DOS) of Mn in the spin-down band at the E_F is larger than that of V, as shown in **Figure S.3**. The AMR ratio for the current (I) along the $MVG_{[100]}$ and $MVG_{[110]}$ directions, respectively, is expressed as

$$AMR^{[100]} = 2C_2^{[100]} \tag{S1}$$

where

$$C_2^{[100]} = \frac{3}{8}\frac{1}{1+r+r_{s,-\to\gamma,-}}\left\{\frac{1}{r+r_{s,-\to\gamma,-}}\left[\left(\frac{\lambda}{\Delta}\right)^2\left(r_{s,-\to\gamma,-}-r_{s,-\to\varepsilon,-}\right)-\left(\frac{\lambda}{H+\Delta}\right)^2 r_{s,-\to\gamma,-}\right]+\left(\frac{\lambda}{H-\Delta}\right)^2 r_{s,+\to\varepsilon,-}\left(r+r_{s,-\to\gamma,-}\right)\right\} \tag{S2}$$

and

$$AMR^{[110]} = 2C_2^{[110]} \tag{S3}$$

where

$$C_2^{[110]} = \frac{3}{8}\frac{1}{1+r+\frac{3}{4}r_{s,-\to\varepsilon,-}+\frac{1}{4}r_{s,-\to\gamma,-}}\left\{\frac{1}{r+\frac{3}{4}r_{s,-\to\varepsilon,-}+\frac{1}{4}r_{s,-\to\gamma,-}}\left[\left(\frac{\lambda}{\Delta}\right)^2\left(r_{s,-\to\varepsilon,-}-r_{s,-\to\gamma,-}\right)-\frac{\lambda^2}{H\Delta}r_{s,-\to\varepsilon,-}+\right.\right.$$

$$\left.\left.\frac{\lambda^2}{\Delta(H+\Delta)}r_{s,-\to\gamma,-}\right]+\frac{\lambda^2}{H(H-\Delta)}r_{s,+\to\varepsilon,-}\left(r+\frac{3}{4}r_{s,-\to\varepsilon,-}+\frac{1}{4}r_{s,-\to\gamma,-}\right)\right\} \quad \text{(S4)}$$

The parameters used in these expressions are as follows: λ = 0.0109 eV is the spin–orbit coupling constant for Mn, H = 2 eV is the exchange field estimated from the energy difference in the peak positions between the spin-up and spin-down of the partial Mn d-DOS, and Δ = 0.6 eV is the energy difference in the peak positions between the ε and γ orbitals of the partial Mn d-DOS induced by the crystal field, **Fig. S3a**. The other parameters, r, $r_{s,+\to\varepsilon,-}$, $r_{s,-\to\varepsilon,-}$, and $r_{s,-\to\gamma,-}$ are defined as $r=\frac{\rho_{s,-}}{\rho_{s,+}}=\left(\frac{m_-^*}{m_+^*}\right)^4\left(\frac{D_+^{(s)}}{D_-^{(s)}}\right)^2$, $r_{s,+\to\varepsilon,-}=\frac{\rho_{s,+\to\varepsilon,-}}{\rho_{s,+}}=\beta_+\frac{D_{\varepsilon,-}^{(d)}}{D_+^{(s)}}$, $r_{s,-\to\varepsilon,-}=\frac{\rho_{s,-\to\varepsilon,-}}{\rho_{s,+}}=r\beta_-\frac{D_{\varepsilon,-}^{(d)}}{D_-^{(s)}}$, $r_{s,-\to\gamma,-}=\frac{\rho_{s,-\to\gamma,-}}{\rho_{s,+}}=r\beta_-\frac{D_{\gamma,-}^{(d)}}{D_-^{(s)}}$. Here, r is the resistivity ratio of the s–s scattering for the spin-down over the s–s scattering for the spin-up, and $r_{s,\sigma\to m,-}=\frac{\rho_{s,\sigma\to m,-}}{\rho_{s,+}}$ is the resistivity ratio of the s–d scattering from the s state with the σ spin to the m orbital with the spin-down over the s–s scattering for the spin-up. The effective mass of the conduction electrons with the σ spin, m_σ^*, is estimated from the calculated energy dispersion diagrams, and its ratio, between the spin-down and the spin-up is estimated as $\frac{m_-^*}{m_+^*}=1$. The amount of partial DOS at the E_F for the n state of the m orbital with the σ spin, $D_{m,\sigma}^{(n)}$, is obtained from the calculated DOS as follows: $D_+^{(S)}=0.00112$, $D_-^{(S)}=0.011$, $D_{\gamma,-}^{(d)}=0.259$, and $D_{\varepsilon,-}^{(d)}=0.372$. The uncertainty parameter with the σ spin, β_σ, was set as $\beta_+=\beta_-=0.1$ depending on impurities and phonons [3].

Figure S4a shows the calculated AMR$^{[110]}$ ratio as a function of $\left(D_{\varepsilon,-}^{(d)}-D_{\gamma,-}^{(d)}\right)/D_{\gamma,-}^{(d)}$ and the contributions from the first (red), second (blue), third (yellow), and fourth (green) terms in

(S4). The first term determines the monotonically decreasing trend because $\left(r_{s,-\to\gamma,-} - r_{s,-\to\varepsilon,-}\right)$ in the first term is proportional to $\left(D_{\gamma,-}^{(d)} - D_{\varepsilon,-}^{(d)}\right)$. In addition, $(1/\Delta)^2$ in the first term with small Δ means that the first term has the large contribution. Similar to the AMR[110], the first term (red) in AMR[100] also determines the monotonically increasing trend, **Fig. S.4b**, as $\left(r_{s,-\to\varepsilon,-} - r_{s,-\to\gamma,-}\right)$ in the first term is proportional to $\left(D_{\varepsilon,-}^{(d)} - D_{\gamma,-}^{(d)}\right)$, and $(1/\Delta)^2$ means the large contribution. The $\left(D_{\varepsilon,-}^{(d)} - D_{\gamma,-}^{(d)}\right)/D_{\gamma,-}^{(d)}$ value is calculated to be 0.435, which results in positive AMR[110] and negative AMR[100] ratios, respectively.

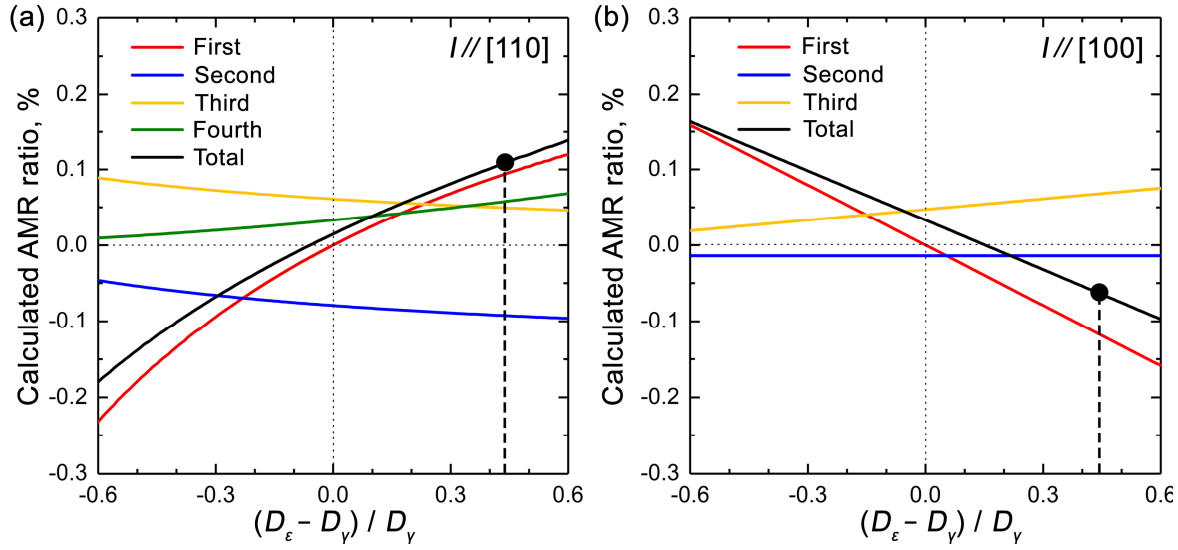

Fig. S.4. The calculated AMR ratio as a function of $\left(D_{\varepsilon,-}^{(d)} - D_{\gamma,-}^{(d)}\right)/D_{\gamma,-}^{(d)}$ for the current along (a) $[110]_{MVG}$, and (b) $[100]_{MVG}$ directions, respectively. The contributions from individual terms in Eq. (S2) and Eq. (S4) are also shown. The dashed lines represent the values obtained from the DOS calculation in Fig. S.2.

References

[1] M. Gutsche, H. Kraus, J. Jochum, B. Kemmather, G. Gutekunst, Growth and characterization of epitaxial vanadium films, Thin Solid Films 248 (1994) 18-27.

[2] R.W.H. Webster, M.T. Scott, S.R. Popuri, J.W.G. Bos, D.A. MacLaren, Epitaxial vanadium nanolayers to suppress interfacial reactions during deposition of titanium-bearing Heusler alloys on MgO(001), Appl. Surf. Sci. 512 (2020) 145649.

[3] S. Kokado, Y. Sakuraba, M. Tsunoda, Spin polarization ratios of resistivity and density of states estimated from anisotropic magnetoresistance ratio for nearly half-metallic ferromagnets, Jpn. J. Appl. Phys. 55 (2016) 108004.